ISSN 2616-5775 Vol. 5, Issue 12: 15-21, DOI: 10.25236/AJCIS.2022.051203

Method for shield tunnel cross-section curve reconstruction based on FBG sensors and neural network

Tipeng Zheng

School of Information Science and Engineering, Chongqing Jiaotong University, Chongqing, 400074, China
chengs.love@163.com

Abstract: *To improve the accuracy of reconstructing morphology in shield tunnel monitoring by fiber-optic Bragg grating (FBG) sensors, a Transformer network-based optimized tunnel cross-sectional curve reconstruction method is proposed to solve the problem of low reconstruction accuracy due to the cumulative error of discrete curvature points. In this research, the optimization method uses all interpolation points as initial points to minimize the cumulative error in fitting the curve with discrete curvature points. Simulation model experiments of the shield tunnel were carried out to verify the accuracy of the optimization method in reconstructing the tunnel section curve. The results show that the shield tunnel simulation model experiments, more accurate tunnel section reconstruction curves were obtained using this optimization method, increasing reconstruction accuracy by 27.3424%.*

Keywords: *Shield tunnel; FBG sensor; Curve reconstruction; Neural networks*

1. Introduction

With the rapid development of China's transport network in recent years, the shield method of tunnel construction has become the most common method due to its advantages in terms of construction safety and speed of excavation. However, after a long period of construction, more and more shield tunnels are being built and put into service. Consequently, the structural health of shield tunnels during operation has become an issue of concern to tunnel managers. Due to the geological environment of the shield tunnel, seismic hazards, structural fatigue, and other adverse factors, the tunnel structure inevitably suffers from morphological deformation. When the accumulated deformation of shield tunnels reaches a certain level, it can lead to the decay of the shield tunnel resistance and the spread of cracks, which can affect the structural health of the shield tunnel tube during the operational phase and lead to safety incidents in tunneling operations. Therefore, it is imperative to monitor the changes quickly and effectively in tunnel structure morphology. Fiber-optic sensor measurement uses sensors to collect information about a deformed object. Its working principle sends an optical signal to a modulator through an optical fiber. After interacting with the parameters to be measured, the optical properties of the optical signal will change and become the source of the modulated signal, which is then sent to a light detector to obtain the measured parameters through a demodulation algorithm. FBG sensors are widely used and have achieved good results in the morphological monitoring of small and high-precision equipment in aerospace, industry, and medical devices [1-3]. In 1993, researchers at the University of Toronto, Canada, first applied fiber optic sensor measurement to bridge monitoring [4]. Nowadays, FBG sensors are used for monitoring large civil engineering projects such as buildings and tunnels [5-7]. Shahriar Sefati et al. optimized the morphological reconstruction curves of FBG for objects with large curvature using artificial neural networks. They compared them with the conventional method, and the results showed that the performance of the reconstruction curves optimized using artificial neural networks was better than the conventional method [8]. Gongyu Hou et al. monitored tunnel cross-section deformation using distributed fiber optic sensors combined with neural network optimization [9].

Although the above studies optimize the discrete curvature point fitting curve and minimize the error in fitting the tunnel profile through neural networks, these studies only focus on and reconstruct the local tunnel profile information, not the overall tunnel profile. In assessing overall tunnel safety, the local morphological information does not reflect the actual general morphological changes in the tunnel. Therefore, there is a risk of misjudgment in using it as a basis for the overall tunnel safety assessment. In this regard, reconstructing the tunnel profile's general morphology is imperative. However, the

ISSN 2616-5775 Vol. 5, Issue 12: 15-21, DOI: 10.25236/AJCIS.2022.051203

accuracy of the discrete curvature points required to close the curve fitted by recursion of the discrete curvature points in reconstructing the overall morphology of the tunnel section is exceptionally high. Therefore, this request cannot meet it in general engineering projects. To solve the problem of excessive reconstruction curve error due to the accumulated error of the discrete curvature point fitting curve and to improve the monitoring accuracy of the fitted tunnel section curve, this research proposes a curvature reconstruction curve optimization method based on Transformer neural network [10]. Finally, a shield tunnel Simulation model experiment is carried out to verify the accuracy of the proposed method in the scaled section model presented in this research.

2. Curvature Offset Correction Method

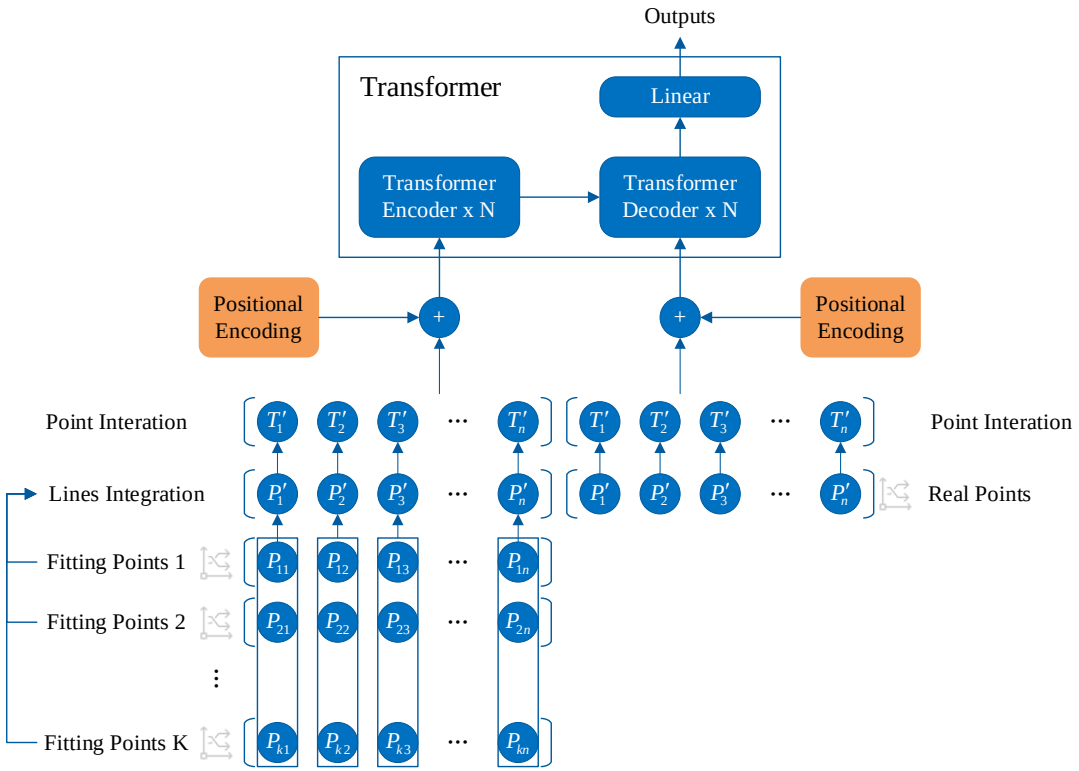

Figure 1: Transformer network sketch.

As the discrete point curvature fitting curve is obtained by the recurrence of curvature information from each point in turn, there is a cumulative error. Moreover, in actual engineering applications, there are inevitable fluctuations in the readings of each sensor, so the reconstruction curve needs to be corrected for offsets. Therefore, the method sets each insertion point in turn as the initial insertion point for curve fitting and compares many curves fitted by different initial points with the actual curve training through the Transformer neural network to obtain the weight relationship between the curves fitted by different initial points, to obtain the final fitted curve. The network sketch is shown in Figure 1. In this research, the same position data of each initial insertion point at the exact moment is normalized and passed into the Transformer encoder with position information. Then the actual coordinate point values are given to the Transformer decoder with position information. The Transformer network is then trained to obtain the possible values of each point.

2.1. Background: Self-attention in Transformer

The Transformer neural network uses an encoder-decoder structure, which extracts target features by stacking encoders and decoders to obtain target relationships. Each encoder and decoder layer comprises a self-attention sub-layer and a feed-forward network sub-layer interconnected by residuals. The network's internal structure is shown in Figure 2.

ISSN 2616-5775 Vol. 5, Issue 12: 15-21, DOI: 10.25236/AJCIS.2022.051203

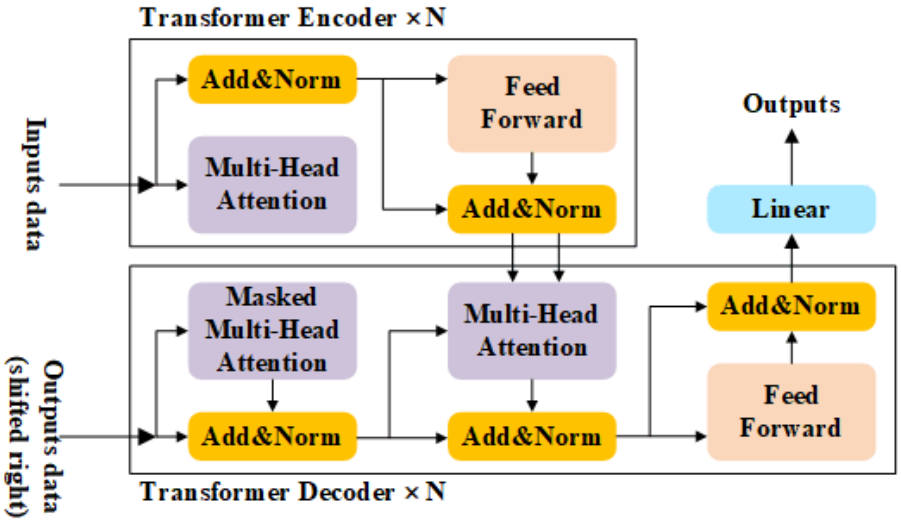

Figure 2: The Transformer neural network internal structure.

The self-attention sub-layer maps the incoming vector to a query and a key-value pair output according to the self-attention function and obtains the attention at the corresponding position by weighting the computation. This is done by first transforming a sequence of M N-dimensional vectors X into a query matrix $Q = XW_{N\times N}^{Q}$, a key matrix $K = XW_{N\times N}^{K}$ and a value matrix $V = XW_{N\times N}^{V}$ by means of the $W_{N\times N}^{Q}$, $W_{N\times N}^{K}$ and $W_{N\times N}^{V}$ matrix transformations, respectively. Each of the query matrix Q, key matrix K and value matrix V is then divided into multi-head attention of H, each with dimension $N_h = N / H$, by focusing on the correlation between each point and outputting a vector of multi-head attention Y^h.

$$Y^h = \text{Attention}(Q^h, K^h, V^h) = \text{Softmax}(\frac{Q^h K^{hT}}{\sqrt{N_h}})V^h \tag{1}$$

The feed-forward network sub-layer combines and linearly transforms the results of each multi-head attention output to obtain a $M \times N$ result matrix Y,

$$Y = \text{RELU}(YW_1 + b_1)W_2 + b_2 \tag{2}$$

Where W_1, b_1, W_2, b_2 are the weight and deviation matrices of the two fully connected layers, respectively. The Multi-head Attention flow chart is shown in Figure 3.

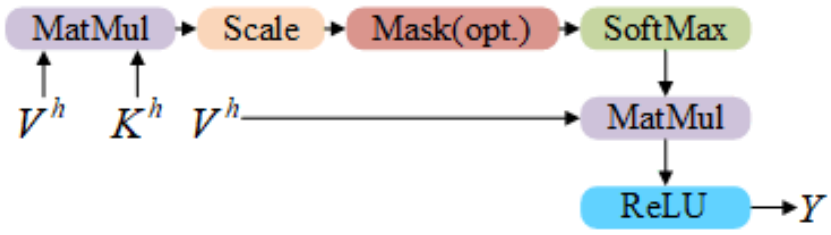

Figure 3: The Multi-head Attention flow chart.

2.2. Extracting the information features of each fitted point

In order to sort out the relationship between curves obtained from multiple initial points, this research passes the information of each curve's corresponding point into the fully connected layer. It gets each curve's weight based on the data training, as shown in Figure 4(a). Similarly, this method uses the fully connected layer to process information for each point to obtain the summation information for that point, as shown in Figure 4(b).

ISSN 2616-5775 Vol. 5, Issue 12: 15-21, DOI: 10.25236/AJCIS.2022.051203

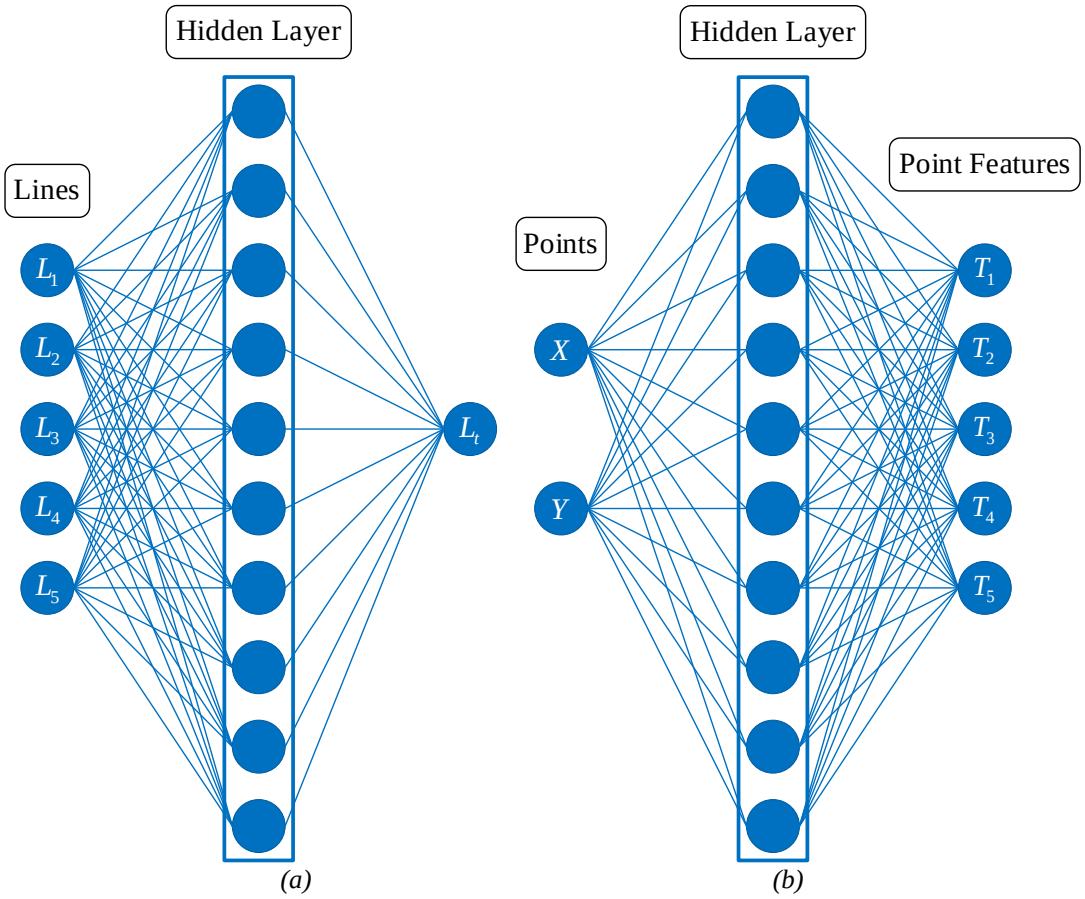

Figure 4: Extracting the information features: (a) Extracting line features; (b) Extracting point's features.

3. Shield tunnel simulation model section curve fitting experiment

3.1. Introduction to the simulation model of the shield tunnel

This experiment takes a river crossing shield tunnel as the background. The river crossing shield tunnel comprises reinforced concrete segments with a strength grade of C60. The outer diameter is 15.2m, the inner diameter is 13.9m, the segment thickness is 0.65m, and the segment ring width is 2m. The author uses ANSYS to establish a numerical simulation model and applies the typical load of the shield tunnel environment and the limit load in case of emergency. Generally, the main forces of a shield tunnel can be divided into water pressure, soil pressure, and soil resistance. In the simulation experiment, applying uniform force on the outer surface of the model segment is equivalent to water pressure, applying vertical pressure is equivalent to soil pressure, and applying transverse load is equivalent to soil resistance. The ratio of layer pressure to soil resistance is 1:0.5. Finally, the shape information of the shield tunnel section under each load is obtained. The model is shown in Figure 5. Specific loads are shown in Table 1.

Table 1: Limit loads for each working condition.

Test	Simulation hydraulic load	Simulation soil load	Simulation soil resistance
1	2 MPa	2 MPa	1 MPa
2	5 MPa	3 MPa	1.5 MPa

ISSN 2616-5775 Vol. 5, Issue 12: 15-21, DOI: 10.25236/AJCIS.2022.051203

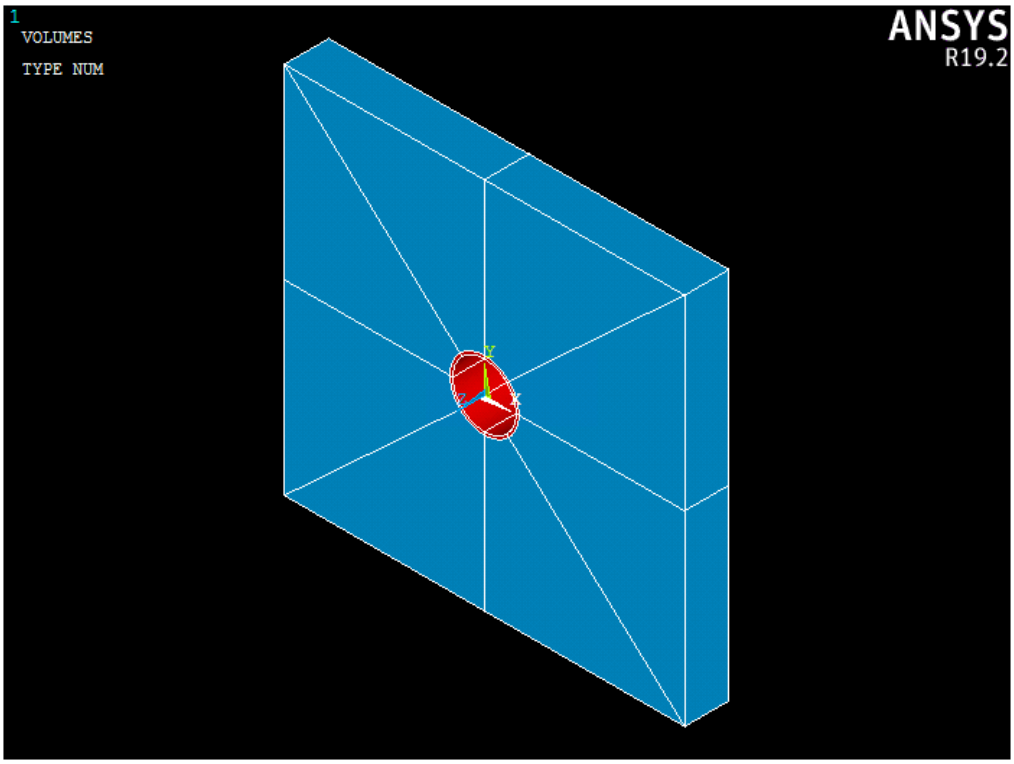

Figure 5: Shield tunnel simulation model.

3.2. Result and Discussion

The Transformer network was used to optimize the fitted curve, obtain the reconstruction curve of the simulation tunnel model cross-section, and compare it with the reconstruction curve without optimization. Meanwhile, to evaluate the curve fitted by discrete point curvature, this research uses the root mean square error formula, which visually reflects the difference between the fitted curve and the actual curve, to evaluate the error of the fitted curve. Finally, this research selects the maximum load for each working condition for visualization in Figure 6. Reconstruction errors before and after calibration for different working conditions are shown in Table 2.

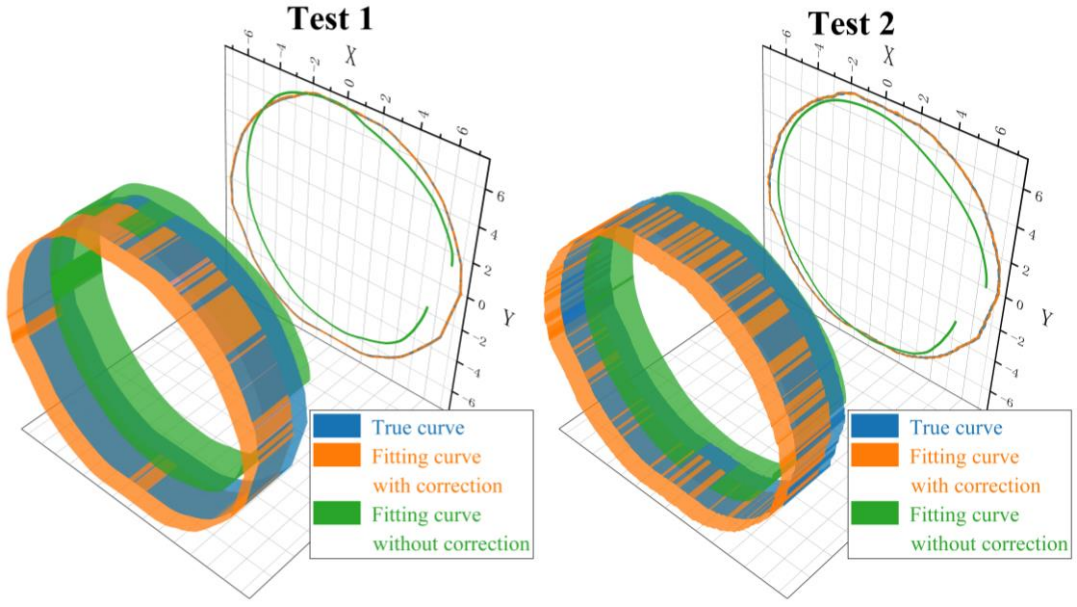

(a) *(b)*

Figure 6: Comparison of curvature recursion fitted curve and simulation tunnel section curve: (a) Test 1 maximum load; (b) Test 2 maximum load.

ISSN 2616-5775 Vol. 5, Issue 12: 15-21, DOI: 10.25236/AJCIS.2022.051203

$$\mathrm{RMSE} = \frac{\sum_{i=0}^{n} \sqrt{(x_i - \overline{x})^2 + (y_i - \overline{y})^2}}{n} \tag{3}$$

Table 2: The compared results with learning-based for curvature offset correction.

Test	RMSE			
	without corrections		with corrections	
	Average [mm]	Max [mm]	Average [mm]	Max [mm]
1	115.5252	223.7604	**1.7228**	**2.9124**
2	138.5234	382.9287	**1.8229**	**2.9967**

Using the calibration method, the average error of the tunnel cross-section reconstruction curve is reduced by 27.3424%, and the maximum error is reduced by 93.3016%. After using the calibration method, the tunnel cross-section reconstruction curve error is significantly reduced. The experimental results show that the proposed recursive curve fitting method based on Transformer network optimization of discrete point curvature can effectively improve the reconstruction accuracy of tunnel section curves and provide a more reliable basis for assessing the safety of shield tunnels. Finally, this study's shield tunnel section optimization fitting method was compared with the ANN [9] and PNN [11]. The final results are shown in Table 3.

Table 3: RMSE comparison of the proposed method and other algorithms.

Test	Approach	RMSE	
		Average [mm]	Max [mm]
1	ANN	7.8176	9.0562
	PNN	4.6580	6.3354
	Ours	**1.7228**	**2.9124**
2	ANN	8.0247	9.1437
	PNN	4.5523	6.8983
	Ours	**1.8229**	**2.9967**

The fitted curves of the shield tunnel cross-section model by each method meet the deformation monitoring code Level 3 standard of the Code for Deformation Measurement of Building and Struct [12], with an error of $\Delta d \leq 10mm$ in displacement observation. Furthermore, the optimized fitting method proposed in this study can meet the deformation monitoring code level 2 standard $\Delta d \leq 3mm$ in the Code for Deformation Measurement of Building and Struct. As a result, the method in this research can obtain more accurate shield tunnel section morphology, providing tunnel managers with better data to support the structural morphology of shield tunnels.

4. Conclusion

This research presents a Transformer network-based method for optimizing discrete point curvature fitted curves. Precisely, the optimization method fits the curves with multiple starting curvature points and integrates the information from each fitted curve by extracting the information from the transformer neural network to obtain an approximation of the actual curve. The overall morphology of the shield tunnel section reconstructed by the optimization method presented in this paper provides a better indication of the shield tunnel's overall morphology than the shield tunnel's local morphology. Therefore, it provides a better basis for the safety assessment of the shield tunnel. The results of this study lead to the following conclusions:

1) In this research, the optimization method of fitting curves with discrete curvature points is compared with the traditional curvature fitting curve optimization method, and the error of the fitted curves is smaller and closer to the actual object curves, which verifies the feasibility of the optimization method in practical application.

2) By comparing the effects of different neural networks on the optimization method, this research demonstrates that transformer neural networks can achieve better optimization performance with the same training.

3) The optimization method can be used to fit the shield tunnel cross-section more accurately, with an average error rate of 0.6981% and a maximum error rate of 3.4072% between the maximum error point and the corresponding point of the actual profile, giving an accuracy of 99.3019% in fitting the

ISSN 2616-5775 Vol. 5, Issue 12: 15-21, DOI: 10.25236/AJCIS.2022.051203

tunnel cross-section and meets the Deformation Monitoring Code Level 2 of the Code for Deformation Measurement of Building and Struct, i.e., each single measurement point error $\Delta d \leq 3mm$.

References

[1] Liu, M., Zhang, X., Song, H., Zhou, S., Zhou, Z. and Zhou, W. (2018). Inverse finite element method for reconstruction of deformation in the gantry structure of heavy-duty machine tool using FBG sensors. Sensors, 18(7), 2173.

[2] Jäckle, S., Strehlow, J. and Heldmann, S. (2019). Shape sensing with fiber Bragg grating sensors. In Bildverarbeitung für die Medizin 2019 (pp. 258-263). Springer Vieweg, Wiesbaden.

[3] Li, T., Qiu, L. and Ren, H. (2019). Distributed curvature sensing and shape reconstruction for soft manipulators with irregular cross sections based on parallel dual-FBG arrays. IEEE/ASME Transactions on Mechatronics, 25(1), 406-417.

[4] Inaudi, D. (2001). Application of optical fiber sensor in civil structural monitoring. In Smart Structures and Materials 2001: Sensory Phenomena and Measurement Instrumentation for Smart Structures and Materials (Vol. 4328, pp. 1-10). SPIE.

[5] Fernando, C., Bernier, A., Banerjee, S., Kahandawa, G. G. and Eppaarchchi, J. (2017). An investigation of the use of embedded FBG sensors to measure temperature and strain inside a concrete beam during the curing period and strain measurements under operational loading. Procedia Engineering, 188, 393-399.

[6] Song, X. and Liang, D. (2018). Dynamic displacement prediction of beam structures using fiber bragg grating sensors. Optik, 158, 1410-1416.

[7] Li, Y., Wang, H., Cai, W., Li, S. and Zhang, Q. (2020). Stability monitoring of surrounding rock mass on a forked tunnel using both strain gauges and FBG sensors. Measurement, 153, 107449.

[8] Sefati, S., Gao, C., Iordachita, I., Taylor, R. H. and Armand, M. (2020). Data-driven shape sensing of a surgical continuum manipulator using an uncalibrated fiber Bragg grating sensor. IEEE sensors journal, 21(3), 3066-3076.

[9] Hou, G. Y., Li, Z. X., Hu, Z. Y., Feng, D. X., Zhou, H. and Cheng, C. (2021). Method for tunnel cross-section deformation monitoring based on distributed fiber optic sensing and neural network. Optical Fiber Technology, 67, 102704.

[10] Vaswani, A., Shazeer, N., Parmar, N., Uszkoreit, J., Jones, L., Gomez, A. N. and Polosukhin, I. (2017). Attention is all you need. Advances in neural information processing systems, 30.

[11] Naghavi, F. and Tavakoli, H. R. (2022). Probabilistic prediction of failure in columns of a steel structure under progressive collapse using response surface and artificial neural network methods. Iranian Journal of Science and Technology, Transactions of Civil Engineering, 46(2), 801-817.

[12] JGJ8-2007(2007), The Code for Measuring Building Deformation.